

ChemComm

Accepted Manuscript



This is an *Accepted Manuscript*, which has been through the Royal Society of Chemistry peer review process and has been accepted for publication.

Accepted Manuscripts are published online shortly after acceptance, before technical editing, formatting and proof reading. Using this free service, authors can make their results available to the community, in citable form, before we publish the edited article. We will replace this *Accepted Manuscript* with the edited and formatted *Advance Article* as soon as it is available.

You can find more information about *Accepted Manuscripts* in the [Information for Authors](#).

Please note that technical editing may introduce minor changes to the text and/or graphics, which may alter content. The journal's standard [Terms & Conditions](#) and the [Ethical guidelines](#) still apply. In no event shall the Royal Society of Chemistry be held responsible for any errors or omissions in this *Accepted Manuscript* or any consequences arising from the use of any information it contains.

Cite this: DOI: 10.1039/c0xx00000x

www.rsc.org/xxxxxx

ARTICLE TYPE

A Dimensionally Stable and Fast-Discharging Graphite-Silicon Composite Li-ion Battery Anode Enabled by Electrostatically Self-Assembled Multifunctional Polymer-Blend Coating

Fu-Sheng Li^a, Yu-Shiang Wu^b, Jackey Chou^c, and Nae-Lih Wu^{*d}⁵ Received (in XXX, XXX) Xth XXXXXXXXXX 20XX, Accepted Xth XXXXXXXXXX 20XX

DOI: 10.1039/b000000x

A high-performance graphite-Si composite anode for Li-ion batteries containing Si nanoparticles (NPs) attached onto graphite microparticles was synthesized by adopting a polymer-blend of poly(diallyl dimethyl-ammonium chloride) and poly(sodium 4-styrenesulfonate). The polymer-blend enabled uniform distribution of Si NPs during synthesis and served as a robust artificial solid-electrolyte interphase that substantially enhanced the cycle stability and rate performance of the composite electrode. The electrode exhibited a specific capacity of 450 mAh g⁻¹, 96% capacity retention at 10 C-rate, 95% retention after 200 cycles, and the same electrode expansion behavior as a pristine graphite electrode.

Advanced Li-ion batteries (LIBs) have been developed to have high capacity density, long cycle life, and high-rate performance for portable electronics, electric vehicles (EVs), and renewable energy storage. Graphite is currently the predominant anode material for commercial LIBs because it has a low cost, low charge/discharge plateau potential, satisfactory specific capacity (372 mAh g⁻¹), and substantially high dimensional stability; its essential role in high-energy LIBs is expected to continue. LIBs employ nearly spherical or potato-shaped, micron-sized graphite particles to achieve high packing density.¹ Si is a potential Li-insertion anode material that has a substantially higher capacity (3579 mAh g⁻¹, corresponding to the formation of Li₁₅Si₄ at room temperature)² than graphite but is susceptible to large (>300% when fully lithiated) volume expansion. The cyclic dimensional variations during charge/discharge cycles result in pulverization and electrical disconnection from the conductive paths of the Si active materials,³ leading to rapid capacity reduction during the cycles. Although the capacity diminishing problems of loosely packed Si nanoparticle (NP) anodes have been substantially improved, low volumetric capacity density and excessive electrode expansion, which cause battery cells to swell, remain as major obstacles to the practical application of Si-dominant anodes.⁴ Composite anodes primarily comprising graphite and a few percent of Si or Si oxide have been recognized as a favorable intermediate product for next-generation high-energy LIBs before the application of Si-dominant anodes is realized.⁵

In this study, a unique Si-on-graphite (Si@G) anode material containing uniformly distributed Si NPs on graphite

microparticles (MPs) was synthesized to address the electrode expansion problem. The concept was to take advantage of the voids between the graphite MPs to provide room for the volume expansion of the Si NPs such that the volumetric change of the entire electrode is maintained close to that of a pristine graphite electrode. This approach was realized by adopting a multifunctional polymer blend consisting of poly(diallyl dimethylammonium chloride) (PDDA) and poly(sodium 4-styrenesulfonate) (PSS) (Fig. S1, ESI[†]), which enabled uniform distribution of Si NPs and substantially enhanced the cycle stability of the electrode.

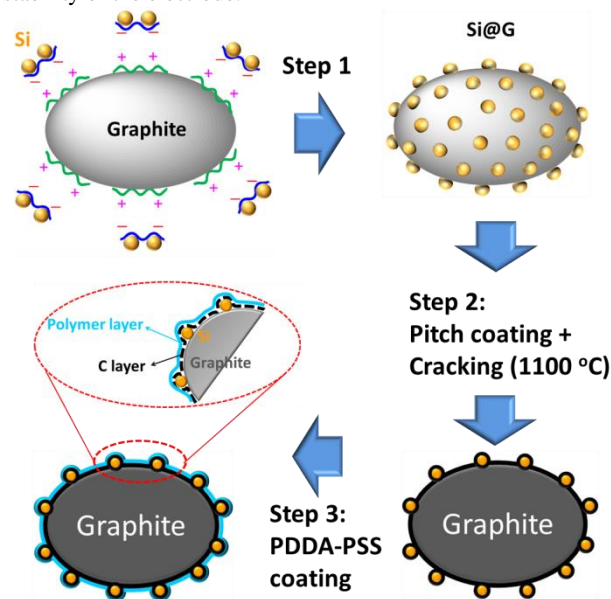


Fig. 1. Schematics showing the synthesis process of the polymer-carbon coated Si-on-graphite (P&C-Si@G) powder.

The synthesis process is schematically shown in Fig. 1 with detailed experimental procedures and conditions described in (S2, ESI[†]). NPs easily segregate because of van der Waals attraction forces. To prevent segregation of the Si NPs, the Si NPs and graphite MPs were respectively coated with PSS and PDDA in the first step. These particles became surface-charged when dispersed in an aqueous solution because of dissociation of the polymer salts. While the negatively charged Si NP particles

tended to repel one another, they were attracted to and bonded with the positively charged graphite MPs. In the second step, the resulting Si@G particles were subjected to a thin pitch coating followed by a high-temperature (1100 °C) treatment where the polymers and pitch coating were cracked to produce a conducting carbon (C) layer on both Si and graphite surfaces. It is worth mentioning that the process of cracking the pitch coating is routinely adopted in the manufacturing of the state-of-the-art graphite MP anodes, and the C-coating is intended to mitigate exfoliation of graphite electrodes in propylene carbonate (PC)-containing electrolytes. In the third step, the resulting C-coated composite was finally coated with a PDDA-PSS layer. For brevity, the Si@G particles coated with C and polymer-C double coatings are referred to as C-Si@G and P&C-Si@G, respectively.

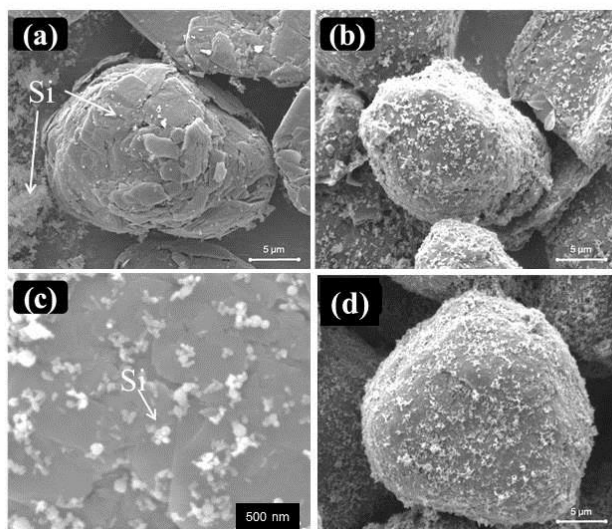


Fig. 2. SEM micrographs showing (a) graphite MPs and segregated Si NPs by conventional mixing (without polymer pre-treatment); (b)(c) uniformly distributed Si NPs on graphite by polymer pre-treatment; (d) P&C-Si@G powder in the electrode.

As shown in Fig. 2, mixing without using polymer precoatings resulted in a mixture (denoted as Si/G) containing segregated Si NPs separated from graphite MPs (Fig. 2a). By contrast, precoating with various surface-charged polymer layers on the Si and graphite particles led to relatively uniform distributions of Si NPs on the surfaces of the graphite MPs (Fig. 2b, c). The electrostatically induced binding between the Si and graphite was

so strong that the Si-NP distribution remained unchanged after the Si@G particles underwent the subsequent coating and electrode preparation processes (Fig. 2d). Energy dispersive X-ray analysis detected an average Si content of 4.3 (± 0.2) wt.%. X-ray diffraction analysis of P&C-Si@G particles revealed that the reflection peaks were caused only by the graphite and Si, indicating no silicon carbide formation during the high-temperature cracking process.

The electrodes had an active material loading of ca. 5 mg cm⁻² with a relatively high packing density (ca. 1.2 g cm⁻³). Preparation of the battery cells and the electrochemical test conditions are described in (S2, ESI†). As shown in Fig. 3a, the mixed Si/G and P&C-Si@G electrodes exhibited an additional delithiation plateau between 0.2 and 0.5 V, which is characteristic of Si, and a 24% increase in specific capacity (447 mAh g⁻¹ vs. 359 mAh g⁻¹) compared with the pristine graphite electrode. The capacity of the P&C-Si@G electrode was based on the total mass of graphite, Si, and the coating materials. Subtracting the capacity of the graphite produced a specific capacity of 3046 mAh g⁻¹ for the Si NPs in P&C-Si@G. The Si/G electrode exhibited a rapid capacity loss of ca. 80% of the Si-enabled extra capacity during the first 25 cycles (Fig. 3b); its capacity quickly approached that of the pristine graphite electrode. Improving the dispersion of Si NPs and adding a carbon coating to produce the C-Si@G electrode effectively prevented the rapid capacity loss during initial cycles (Fig. 3b), but the capacity started to reduce quickly after 50 cycles. Applying an additional PDDA-PSS coating led to substantial enhancement in long-term cycling stability; the P&C-Si@G electrode retained 95% total capacity after 200 cycles (Fig. 3b). The capacities contributed by Si in these electrodes were estimated by subtracting the capacity data of the PDDA-PSS-coated graphite electrode, and they are plotted against the cycle number in Fig. 3c. The estimated specific capacity of the Si component in the Si/G electrode lost 68% capacity, from 2383 mAh g⁻¹ to 761 mAh g⁻¹, in 50 cycles, whereas that in the P&C-Si@G electrode remained stable at 2382 mAh g⁻¹ from the 10th cycle to the 200th cycle. Furthermore, compared with the C-Si@G electrode, the P&C-Si@G electrode exhibited superior Coulombic efficiencies in the approximate range of 99.5% to 99.7% during the last 150 cycles (Fig. S3).

Measurement of the electrode thickness after cycling showed that the P&C-Si@G electrode expanded by 18% (Table 1), which was similar to the thickness of the pristine graphite electrode (17%), whereas the Si/G electrode expanded by almost double (33%). The data demonstrated that the present Si-on-G approach

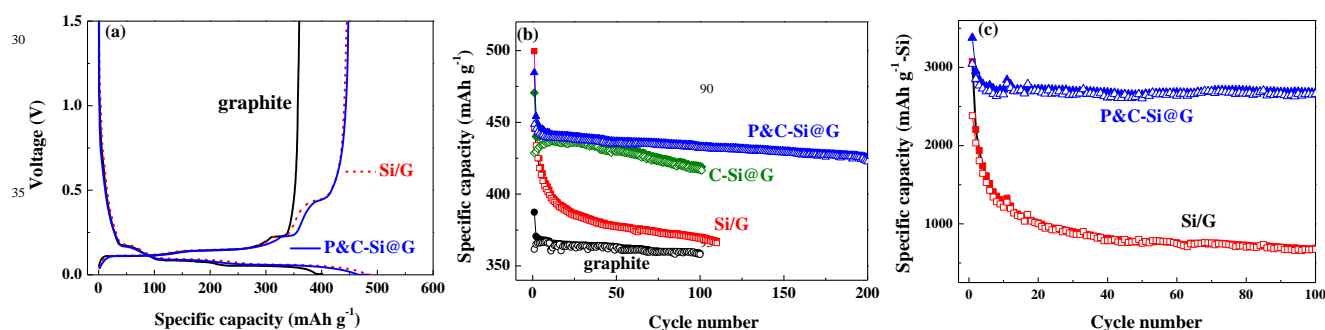


Fig. 3. Comparison in charge/discharge performance among pristine, Si/G, C-Si@G, and P&C-Si@G electrodes. (a) potentials curves; (b) specific capacity of active material versus cycle number; (c) specific capacity of Si component versus cycle number.

succeeded in substantially increasing (24%) the specific capacity of the graphite anode while avoiding excessive electrode expansion.

5 Table 1. Variations in electrode thickness after 100 cycles

thickness	graphite	Si/G	P&C-Si@G
Original (μm) ^a	47	52	50
After cycling	55	69	59
(μm)			
Variation (%)	17%	33%	18%

^aThe thickness values exclude the current-collector (Cu) contribution.

Another outstanding property of the P&C-Si@G composite electrode is its high rate capability. Fig. 4 shows the plot of the delithiation capacity (equivalent to discharge in a full-cell operation) versus C-rate. The P&C-Si@G electrode demonstrated an average capacity of 445 mAh g^{-1} at 0.1 C-rate and retained 96% (426 mAh g^{-1}) of the capacity as the charge rate increased by 100 fold to 10 C-rate. The C-Si@G electrode had the same specific capacity as the P&C-Si@G electrode at 0.1 C-rate but retained only 89% at 10 C-rate. The Si/G electrode exhibited the poorest performance, retaining a capacity of less than 200 mAh g^{-1} .

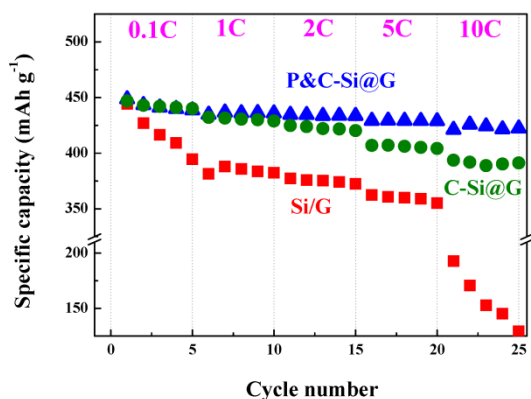


Fig. 4. De-lithiation rate performance. All electrodes are lithiated at 0.1C-rate and de-lithiated at the designated current rates.

The aforementioned electrochemical data indicated two critical functions of the outer PDDA-PSS coating in improving the performance of the C-Si@G electrode. First, the polymer coating provided the composite electrode with long-term cycling stability. This enhancement may be attributable to the ductile characteristic of the polymer coating, which allowed the coating layer to stretch and contract with the dimensional changes of the Si NPs without rupture, thereby allowing the NPs to maintain close contact with graphite MPs. By contrast, because of the brittle nature of the pitch C-coating, it may crack under the stress of the volume expansion of the Si NPs; therefore, it is incapable of holding the NPs. A substantial difference in mechanical robustness between the hard pitch carbon coating and the PDDA-PSS polymeric coating was demonstrated by subjecting the coated powders to a drying mixing in a 3D mixer, where strong collision between particles and between particles and the wall occurred. For the C-

Si@G powder, the surface C-layer of a substantial number of the particles broke and peeled off after the test (Fig. S4). By contrast, all of the P&C-Si@G particles remained unchanged.

The second critical function of the polymer coating is its enhancement of rate performance. As mentioned previously, the P&C-Si@G exhibited higher Coulombic efficiencies throughout the cycling than the C-Si@G electrode did (Fig. S3). The difference suggested that the polymer coating may serve as an artificial solid-electrolyte interphase (SEI) layer to reduce the formation of natural SEI of higher charge-transfer resistance. Ac impedance measurement showed that C-Si@G electrode had a greater overall (thin-film + charge-transfer) resistance than the P&C-Si@G electrode after 100 cycles (Figure S5). SEM analysis of the morphologies of the cycled electrodes also indicated that the cycled C-Si@G electrode had a thicker SEI layer (Figure S6).

In summary, a high-performance Si@G composite anode was synthesized in this study by adopting a PDDA-PSS polymer blend to improve the uniformity of Si NP distribution and serve as a surface coating to enhance cycle stability and rate performance. The composite exhibited the same expansion behavior as the pristine graphite electrode but with substantially enhanced specific capacity and rate performance.

This study was supported by the Ministry of Science and Technology (MOST) (NSC 103-ET -E-002 -001-ET) and the Ministry of Economic Affairs (103-EC-17-A-08-S1-183), Taiwan, R.O.C.. S.-J. Ji of MOST (National Taiwan University) is acknowledged for SEM analysis.

Notes and references

- ^a Department of Chemical Engineering, National Taiwan University, Taipei 106, Taiwan. Fax: +886-2-23627158; Tel: +886-2-23623040; E-mail: nlw001@ntu.edu.tw.
- ^b Department of Mechanical Engineering, China University of Science and Technology, Taipei, 115, Taiwan
- ^c Long Time Technology Corp., Chun-Hsin Rd, New Taipei City, 221, Taiwan
- [†] Electronic Supplementary Information (ESI) available: [chemical formula of polymers; Experimental; Coulombic efficiency; SEM micrographs; ac impedance measurement]
- (a) K. Ohzeki, Y. Saito, B. Golman and K. Shinohara, *Carbon*, 2005, **43**, 1673; (b) H. Buqa, D. Goers, M. Holzapfel, M. E. Spahr and P. Novak, *J. Electrochem. Soc.*, 2005, **152**, A474.
 - (a) M. N. Obrovac and L. Christensen, *Electrochem Solid St*, 2004, **7**, A93; (b) C. M. Park, J. H. Kim, H. Kim and H. J. Sohn, *Chem. Soc. Rev.*, 2010, **39**, 3115.
 - (a) T. D. Hatchard and J. R. Dahn, *J. Electrochem. Soc.*, 2004, **151**, A838; (b) J. Li and J. R. Dahn, *J. Electrochem. Soc.*, 2007, **154**, A156; (c) Y. C. Yen, S. C. Chao, H. C. Wu and N. L. Wu, *J. Electrochem. Soc.*, 2009, **156**, A95; (d) Y. Yu, L. Gu, C. B. Zhu, S. Tsukimoto, P. A. van Aken and J. Maier, *Adv. Mater.*, 2010, **22**, 2247; (e) L. W. Su, Z. Zhou and M. M. Ren, *Chem. Commun.*, 2010, **46**, 2590.
 - (a) B. Hertzberg, A. Alexeev and G. Yushin, *J. Am. Chem. Soc.*, 2010, **132**, 8548; (b) H. Wu and Y. Cui, *Nano Today*, 2012, **7**, 414; (c) X. Su, Q. L. Wu, J. C. Li, X. C. Xiao, A. Lott, W. Q. Lu, B. W. Sheldon and J. Wu, *Adv. Energy Mater.*, 2014, **4**; (d) J. Liu, Q. Zhang, Z. Y. Wu, J. H. Wu, J. T. Li, L. Huang and S. G. Sun, *Chem. Commun.*, 2014, **50**, 6386.
 - (a) N. Dimov, S. Kugino and A. Yoshio, *J. Power Sources*, 2004, **136**, 108; (b) H. Y. Lee and S. M. Lee, *Electrochem. Commun.*, 2004, **6**, 465; (c) X. S. Zhou, Y. X. Yin, L. J. Wan and Y. G. Guo, *Adv. Energy Mater.*, 2012, **2**, 1086; (d) X. S. Zhou, Y. X. Yin, L. J. Wan and Y. G. Guo, *Chem. Commun.*, 2012, **48**, 2198.